

Changes of T_c , J_c , B_{c2} and the lattice parameter of the Nb_3Sn phase formed at the initial stage of growth in a multifilamentary superconductive wire

B. A. GŁOWACKI

Institute of Fundamental Electrotechnics and Electrotechnology, Technical University of Wrocław, Wrocław, PO Box 1318, Poland

Z. BUKOWSKI

Institute for Low Temperature and Structure Research, Polish Academy of Science, Wrocław, PO Box 937, Poland

Investigations were made of the superconducting transition temperature, T_c , the upper critical flux density, B_{c2} , and the critical current density, J_c , of Nb_3Sn layers in filamentary wire in a bronze matrix. The lattice parameter, a_0 , and T_c of Nb_3Sn layers in 259-filament wire were determined after removal of the bronze matrix. The microstructure and layer thickness were studied using scanning electron microscopy. The diffusion formation of Nb_3Sn phase at 1023 K was studied until the complete reaction of the niobium filaments. It was found that the Nb_3Sn layer begins to form in the manufacturing process during the intermediate annealing at 793 K, and that there is a considerable degradation of critical parameters due to the non-stoichiometry of the Nb_3Sn phase in layers thinner than 1 μm .

1. Introduction

Nb_3Sn multifilamentary superconducting wire finds a wide practical application to the generation of high magnetic fields up to 16 T [1]. This type of superconducting wire is produced by the "bronze route" [2] where niobium rods are inserted into holes drilled in a bronze matrix and then drawn. It has been empirically established [3] that the high-tin bronze, 13 wt % Sn, used for Nb_3Sn manufacture needs to be annealed at the temperature of 793 K every three draw passes, the reduction per draw pass being conventionally 20%. After drawing to the final diameter the composite is heat-treated in the temperature range of 927 to 1123 K to form Nb_3Sn around each niobium filament by solid-state reactive diffusion. It has been found that the thermal contraction coefficient of Nb_3Sn is less than that of bronze matrix [4], so during cool-down after the high-temperature heat treatment to liquid helium temperature, the bronze contracts from the niobium filaments and places them in compression. Hillman *et al.*, [2] have shown that T_c increases by one degree for samples in which the entire bronze matrix has been removed by etching and thus reducing the prestress almost to zero. X-ray investigations of the Nb_3Sn phase, performed by Pan *et al.* [5] and Devatay *et al.* [6] have shown that the lattice parameter of this phase changes in the range of 0.5289 nm for samples containing 25 at % Sn, to 0.5281 nm for samples containing less than 19 to 20% Sn. X-ray diffraction studies of reacted Nb_3Sn multifilamentary wires which

had the residual bronze matrix removed by etching, showed the broadening of diffraction lines due to a very small grain size and microstresses [7]. Studies have shown that grain boundaries of the Nb_3Sn are effective pinning centres [8, 9] and are effective in increasing the critical current in Nb_3Sn superconductors [10]. The pinning force, P_v , being the product of the critical current density, J_c , and the macroscopic flux density, B , ($P_v = J_c B$) and thus of J_c , increases with decreasing grain size of the Nb_3Sn layer [10].

Up to the present, many papers have been published to explain the relationship between critical parameters and microstructural properties of the Nb_3Sn phase, yet only a few papers have dealt with the initial stage of the Nb_3Sn layer growth in multifilamentary wires during the stage of Nb_3Sn formation during the wire manufacture [11].

2. Experimental details

2.1. Materials preparation

259-filament wire of full diameter 0.78 mm and average diameter of niobium filaments of 12 μm , fabricated by the bronze route, was used in our investigations [12, 13]. The bronze (13 wt % Sn) to niobium ratio was 15.3 in the unreacted wire. After each 60% reduction, recovery and recrystallization of bronze rods was carried out by annealing in an argon atmosphere at 793 K for 1 h. Samples from the final wire were heated at 1023 K for times between 15 min and 100 h.

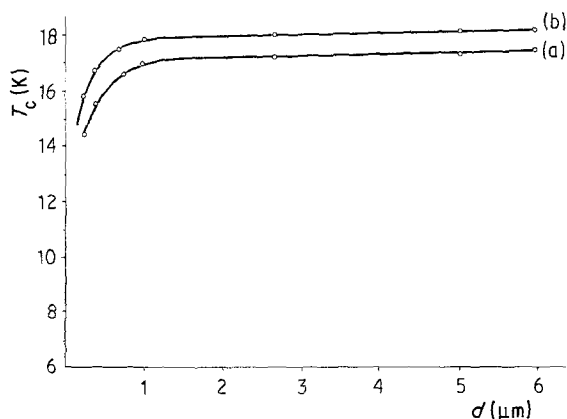


Figure 1 The dependence of the superconducting transition temperature, T_c , on Nb_3Sn layer thickness of a wire (a) in a bronze matrix and (b) without matrix.

2.2. Superconducting transition temperature

T_c was measured with a carbon thermometer and a germanium resistive thermometer [14]. The accuracy of measurements was 0.05 K. T_c was defined as the midpoint of the resistive transition, i.e. the temperature at which the resistance of the sample was half of its normal value.

2.3. Critical current density

J_c measurements were carried out in a perpendicular magnetic field in the range of 0 to 4.25 T at 4.2 K. The electric field criterion, $E = 1 \times 10^{-6} \text{ V cm}^{-1}$, was used to determine J_c [15].

2.4. Upper critical flux density

Hake's empirical formula [16], which can be written in the form

$$B_{c2}(0) = 0.693T_c \left(\frac{dB_{c2}(T)}{dT} \right)_{T=T_c} \quad (1)$$

was used to calculate $B_{c2}(0)$. The slope $[dB_{c2}(T)/dT]_{T=T_c}$ of the $B_{c2}(T)$ curve was determined with an accuracy of 0.5 T K^{-1} .

2.5. Lattice parameters

The lattice parameters of the Nb_3Sn phase in etched specimens was determined using X-ray diffractometer and $\text{CuK}\alpha$ radiation using the (3 2 1) and (4 0 0) lines.

2.6. Microstructure

Investigations of chemical composition and thickness of Nb_3Sn layers were performed on polished cross-

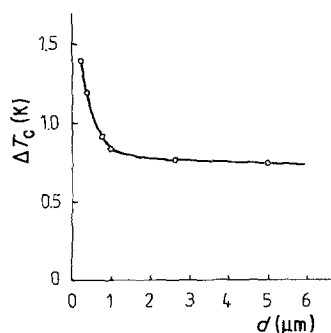


Figure 2 The difference, ΔT_c , between T_c of a wire in a matrix and without matrix as a function of Nb_3Sn layer thickness.

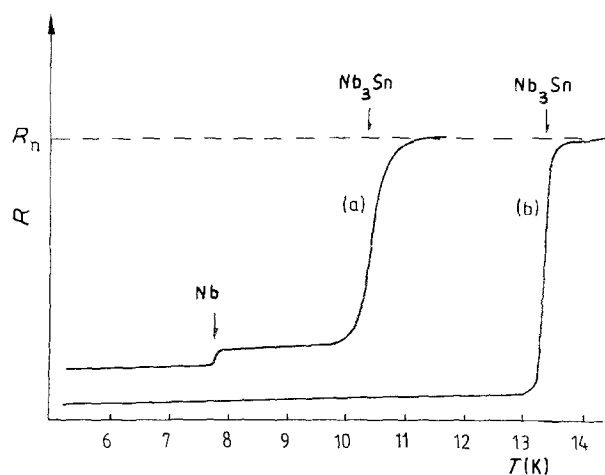


Figure 3 Resistive transitions from the superconducting to normal state: (a) as-drawn wire, 60% reduction; (b) wire annealed 793 K, 1 h.

sections using electron microprobe and SEM. The granular structure of Nb_3Sn layers was observed on the low-temperature fractured surface of the conductor [17]. The microstresses were estimated from the broadening of X-ray diffraction lines [18].

3. Experimental results

3.1. Superconducting transition temperature

Investigations of the dependence of T_c on the thickness of the Nb_3Sn superconducting layer, d , carried out on samples reacted at 1023 K measured with the bronze matrix present and after its removal, showed that in both cases T_c increases with the increase in d (Fig. 1). T_c increases considerably with increase of the layer thickness in the range of 0 to $1 \mu\text{m}$, yet a further increase of d does not, in any significant way, affect T_c . Though the character of the dependence $T_c(d)$ of samples in the bronze matrix and after its removal is similar, measurements of T_c of the wire in the bronze matrix always give lower values for all examined thicknesses of the Nb_3Sn layer until the niobium filaments are completely reacted. The difference between T_c of the wire without the matrix and in the matrix, ΔT_c , as a function of the layer thickness is presented in Fig. 2. As can be seen, T_c decreases considerably with increase of d in the range of 0 to $1 \mu\text{m}$, yet further increase of the layer thickness does not bring about any significant changes of T_c . Examinations of the wire carried out during the manufacturing process showed that the intermediate annealing at 793 K to recrystallize the bronze matrix results in the formation of an Nb_3Sn layer with $T_c = 13.45 \text{ K}$, whereas a wire subject only to the drawing undergoes two superconducting transitions: the first transition at 10.4 K and a second small one at 7.8 K (Fig. 3). It is also found that T_c of the drawn wire not subject to the last recrystallizing annealing does not increase after the removal of the bronze matrix.

3.2. Critical current density

The critical current density as a function of Nb_3Sn layer thickness is presented in Fig. 4. The maximum of the curve $J_c(d)$, for a layer thickness of $\sim 1 \mu\text{m}$,

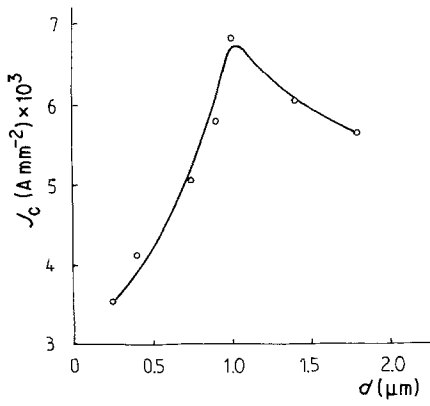


Figure 4 The critical current density, J_c , as a function of superconducting layer thickness, d , for multifilamentary Nb₃Sn.

indicates that some phenomenon markedly reduces J_c , in layers thinner than 1 μm .

3.3. Upper critical field

The dependence of B_{c2} on temperature of the drawn sample and that of the sample annealed at 793 K is presented in Fig. 5. Since the dependence $B_{c2}(T)$ is linear for the measured values of induction, the sample subject to the intermediate annealing satisfies Hake's empirical formula. The initial slope parameter of the annealed sample equalled 2 T K^{-1} and $B_{c2}(0)$, calculated on the basis of Hake's formula, was equal to 18.56 T. Since the variation of B_{c2} with temperature of the drawn sample is parabolic near T_c , it is impossible to determine properly the initial slope parameter $[dB_{c2}(T)/dT]_{T=T_c}$ from Fig. 5. This parameter of samples annealed at 1023 K in a short period of time was also nearly equal to 2 T K^{-1} . Therefore the value of $B_{c2}(0)$ was determined, in accordance with Hake's formula, (Equation 1) by T_c .

3.4. Lattice parameter

The X-ray investigations showed that the lattice parameter of the Nb₃Sn phase increased by 0.5281 to 0.5288 nm with increase of the layer thickness, as shown in Fig. 6. The lattice parameter suddenly increases in the initial stage of growth of the Nb₃Sn layer, but the increase of layer thickness over 1 μm is accompanied by only a slight increase of a_0 .

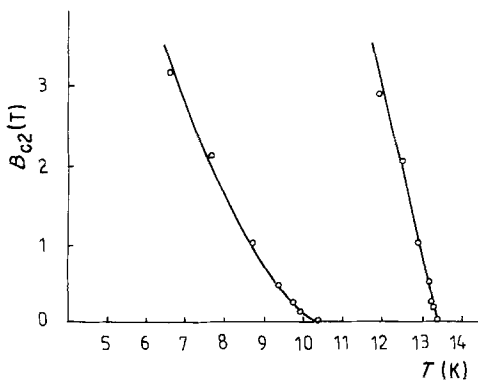


Figure 5 The upper critical flux density B_{c2} , as a function of temperature for multifilamentary Nb₃Sn wire: (a) as-drawn, 60% reduction; (b) annealed, 793 K, 1 h.

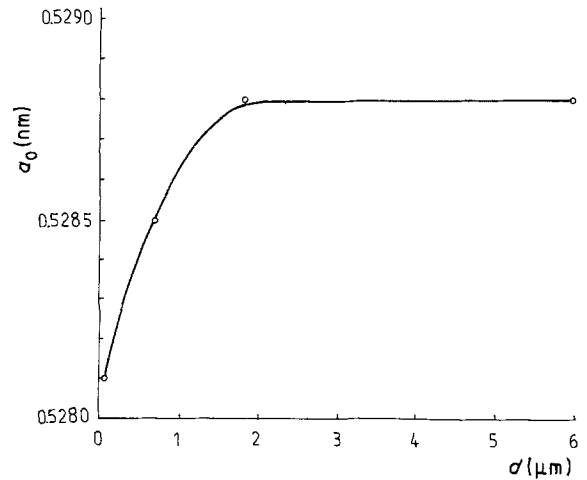


Figure 6 The lattice parameter, a_0 , of Nb₃Sn phase as a function of layer thickness.

3.5. Microstructure

Microstructural examinations of Nb₃Sn layers with the SEM have shown that the grain size of the Nb₃Sn phase increase with the diffusion time (Fig. 7). It has been found that the widths of diffraction lines of the Nb₃Sn phase decrease with the diffusion time, i.e. with the increase of layer thickness (Fig. 8). The half-width, $\Delta 2\theta$, of diffraction line (3 2 1) rapidly decreases in the initial stage of the Nb₃Sn layer growth up to the moment when d is approximately 1 μm thick (Fig. 9).

The broadening of the diffraction line

$$\beta = [\Delta 2\theta^2 - b^2]^{1/2} \quad (2)$$

where b is the instrumental broadening, is affected by the grain size and microstress disorder and this problem has been discussed in detail [18]. In the limiting case, where crystallite size alone is operative, β is given by

$$\beta = \lambda/\varepsilon \cos \theta \quad (3)$$

where λ = X-ray wavelength and ε = effective crystallite size.

A plot of β against $1/\cos \theta$ should be a straight line through the origin. Similarly, if the only cause of broadening is microstress disorder, β will be given by

$$\beta = \frac{4\sigma}{E_{hkl}} \tan \theta \quad (4)$$

where σ = mean stress and E_{hkl} = Young's modulus. A plot of β against $\tan \theta$ should be a straight line through the origin. In order to determine which of these factors exerts a dominant influence on the broadening of diffraction lines of the Nb₃Sn phase formed in the initial stage of growth, $\beta = f(1/\cos \theta)$ and $\beta = f(\tan \theta)$ were plotted for layers 0.7 and 1.8 μm thick. It was found that the broadening of the diffraction lines is caused by microstress disorder, which decreases with the increase of layer thickness.

4. Discussion

4.1. Influence of lattice parameter and matrix stress on T_c

Results of the measurements of a_0 of Nb₃Sn layers presented in Fig. 6 indicate that those layers which

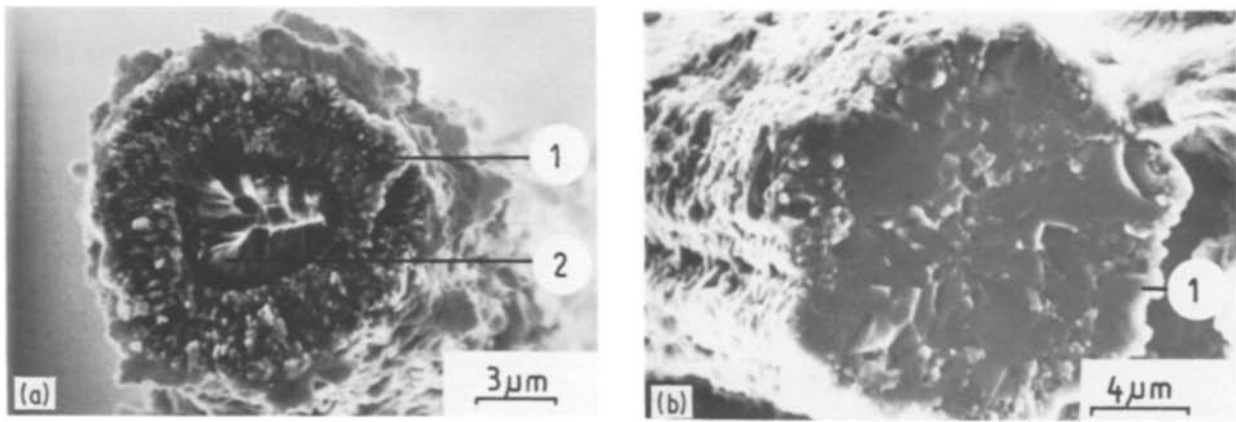


Figure 7 Scanning electron micrograph of fracture of a single filament obtained at 1029 K during (a) 5.33 h, (b) 100 h; 1, Nb₃Sn; 2, Nb.

are thinner than approximately 1 μm are non-stoichiometric and tin-deficient [5, 6]. Those thicker than 1 μm are essentially stoichiometric. The observed decrease of T_c with decreasing superconducting layer thickness below 1 μm, both in the bronze matrix and after its removal, shown in Fig. 1 is due to the increasing departure from stoichiometric composition of the Nb₃Sn phase [5]. Though the character of the dependence $T_c(d)$ of filaments in the bronze matrix and after its removal is similar, the difference ΔT_c , brought about by stresses resulting from the difference between coefficients of thermal contraction of Nb₃Sn and the bronze matrix, decreases considerably with the increase of d up to approximately 1 μm (Fig. 2). The matrix strain decreases with decrease of tin concen-

tration in the bronze [4] and with an increase of the ratio of the volume of Nb₃Sn to the matrix [19]. In our case, during the Nb₃Sn formation the decrease of tin concentration is small in the matrix. This, and the fact that the difference between thermal expansion coefficients of bronze and pure copper is slight, about 3% [4], and that the ratio of Nb₃Sn to the matrix increases almost linearly as a function of Nb₃Sn layer thickness, allow one to conclude that the matrix strain does not undergo radical changes as a function of layer thickness. Therefore the strong decrease of ΔT_c of layers thinner than 1 μm should be attributed to the decreasing departure from stoichiometry of the Nb₃Sn phase and to the decay of microstresses.

4.2. Nb₃Sn formed in the manufacturing process

It is well known that in the manufacturing process, during the reduction of the wire from the initial diameter to the final diameter tens of 60% reductions of the wire diameter are usually realized after each annealing process.

After such composite fabrication, a considerable amount of A15 phase is formed on each niobium filament surface. This phase is formed of a fragmented layer containing irregular grains which has grown during different stages of the manufacturing process. The grains are characterized by different values of critical parameters (T_c , B_{c2}). As drawing the wire breaks the continuity of the Nb₃Sn layer because a superconducting transition of niobium filaments occurs at 7.2 K (Fig. 3), resistive transitions for the

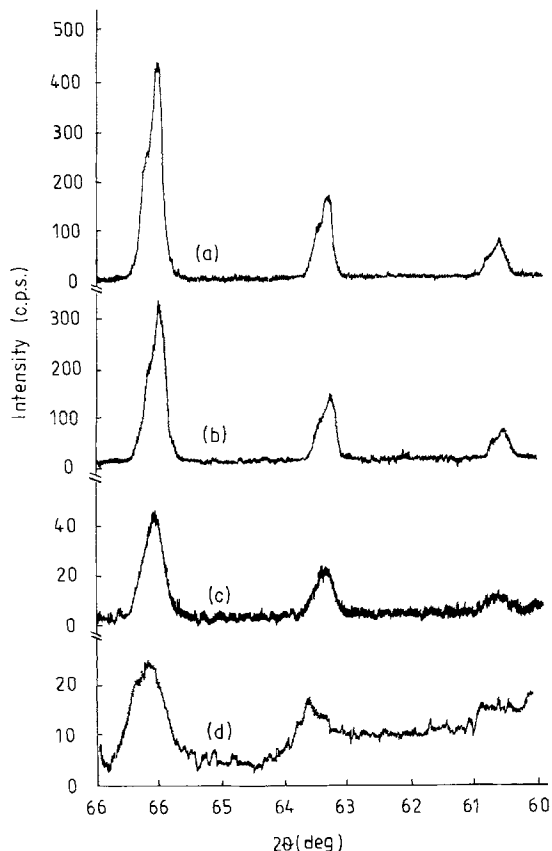


Figure 8 X-ray diffraction profiles of Nb₃Sn diffusion layers formed at different temperatures and times. (a) 1023 K, 28 h; $d = 6 \mu\text{m}$. (b) 1023 K, 2.5 h; $d = 1.8 \mu\text{m}$. (c) 1023 K, 15 min; $d = 0.7 \mu\text{m}$. (d) 793 K, 1 h.

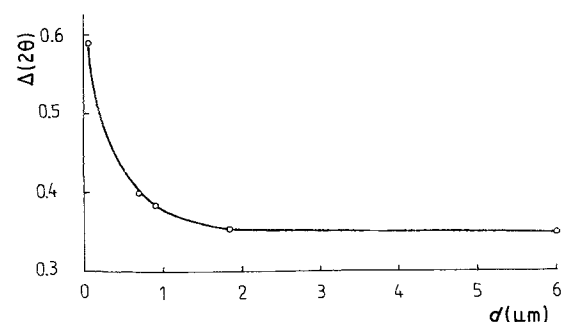


Figure 9 The half-width, $\Delta 2\theta$, of the diffraction line (321) as a function of Nb₃Sn layer thickness.

wire after drawing appeared when the first percolation paths along wire were established. In our case the Nb₃Sn layer of $T_c = 13.45$ K began to form during the intermediate annealing process in the manufacture of the multifilamentary wire. After drawing, T_c of the wire decreased by 13.45 K to 10.4 K and exhibited a broadening of the transition at ~ 1.5 K. This critical temperature does not change after removal of the bronze matrix: this is due to application of strong elastic strains during drawing so that the thermal effect of matrix stress is negligible. That the dependence $B_{c2}(T)$ for this wire does not satisfy Hake's law (Fig. 5) is consistent with the presence of strong deformation in the A15 layer. The positive curvature of B_{c2} against T_c arises from the transition width caused by inhomogeneities. To illustrate this effect one may construct a family of crossing slight lines, tangent to the curve $B_{c2}(T)$, corresponding to a distribution of Nb₃Sn paths with different T_c in the A15 layer.

4.3. Critical current density

It follows from our microscopic observations and from Kwasnitza *et al.* [20] that the increase of Nb₃Sn layer thickness is accompanied by the growth of grain size. According to Scanlan *et al.* [10] the growth of grain size is accompanied by the decrease of pinning force, P_v , and of J_c , and therefore Nb₃Sn layers of the smallest thickness and thus of the smallest grain size should have the greatest J_c . The maximum of the curve $J_c(d)$ for $d \sim 1 \mu\text{m}$ can be attributed to the occurrence of J_c degradation effects in layers thinner than $1 \mu\text{m}$. In order to explain the occurrence of the degradation in J_c we shall consider the influence of the physical parameters of the Nb₃Sn layers thinner than $1 \mu\text{m}$ on the mean difference of free-energy density between the normal state and the mixed one, as well as the "effectiveness of pinning" of flux lines in pinning centres. The mean difference of the free-energy density can be expressed using the Ginzburg–Landau theory [21]:

$$\langle g_m(H, T) - g_n \rangle = - \frac{\mu_0 (H_{c2} - H)^2}{2 (2K^2 - 1)\beta_A}. \quad (5)$$

$$K = K_0 + A\gamma^{1/2}\varrho_n \quad (6)$$

where g_n , g_m = Gibbs free-energy density in the normal state and mixed state, respectively, K = Ginzburg–Landau parameter, K_0 = Ginzburg–Landau parameter of the pure material (which is calculated to be 14 [22]), A = constant, γ = electronic thermal capacity per unit volume, ϱ_n = electrical resistivity in the normal state. Orlando *et al.* [23] have presented detailed analysis of the variation of γ and ϱ_n in Nb₃Sn layers with disorder. From their investigations one can calculate that with a strong increase in ϱ_n (with increasing disorder) γ decreases very slowly so that the value of K increases with increasing disorder. On the basis of Orlando *et al.*'s results and calculation of $[dB/dT]_{T_c}$ as a function of (T_c, ϱ_n) , presented by Esomekh *et al.* [24] one can conclude that variation of T_c with increasing ϱ_n is independent of the means by which the sample is disordered, whether this is by

irradiation of a stoichiometric sample, deviation from stoichiometry or tertiary additions. It follows from our investigations that the thinner Nb₃Sn layer becomes less than $1 \mu\text{m}$, the greater the disorder and microstress occurring in the A15 phase. These disturbances of the structure result in an increase in ϱ_n and a decrease of $\langle g_m(H, T) - g_n \rangle$ (Equations 5 and 6). The value of $B_{c2} = \mu_0 H_{c2}$ calculated on the basis of Hake's formula (Equation 1) also indicates that with decrease of layer thickness below $1 \mu\text{m}$ B_{c2} also decreases, thus reducing $\langle g_m(H, T) - g_n \rangle$. Therefore, if $\langle g_m(H, T) - g_n \rangle$, resulting from the formation of a fluxoid lattice in the mixed state, decreases then the "effectiveness of pinning" of flux lines in pinning centres and the volumetric pinning force density, P_v , decrease thus justifying the greatest degradation of J_c in the thinnest layers, below $1 \mu\text{m}$.

5. Concluding remarks

Formation of an Nb₃Sn layer occurs during intermediate annealing at 793 K. The layer is destroyed during further drawing. The greatest changes of critical parameters and the lattice constant of the Nb₃Sn layer as a function of layer thickness, investigated from the beginning of Nb₃Sn formation up to complete reaction of niobium filaments, occur in layers of thicknesses up to $1 \mu\text{m}$. The degradation of T_c , J_c , and B_{c2} in layers thinner than $1 \mu\text{m}$ is caused by non-stoichiometry and microstresses in the A15 phase.

References

1. B. BOGNER, in "Superconducting Machines and Devices", edited by S. Foner and B. B. Schwartz (Plenum Press, New York, 1974) p. 602.
2. H. HILLMAN, H. PFISTER, E. SPRINGER, M. WILHELM and K. WOHLLEBEN, in "Filamentary A15 Superconductors", edited by M. Suenaga and A. F. Clark (Plenum Press, New York, 1980) p. 17.
3. B. GŁOWACKI, DSc dissertation, Institute for Low Temperature and Structural Research, Polish Academy of Science (1983).
4. D. S. EASTON, D. M. KROEGER, W. SPECKING and C. C. KOCH, *J. Appl. Phys.* **51** (1980) 2748.
5. V. M. PAN, Yu. J. BELETSKII and V. J. LATYSH-EVA, *Metally* **5** (1977) 220.
6. H. DEVATAY, J. L. JORDA, M. DECROUX, J. MULLER and R. FLUKIGER, *J. Mater. Sci.* **16** (1981) 2145.
7. R. FLUKIGER, W. SCHAUER, W. SPECKING, B. SCHMIDT and E. SPRINGER, *IEEE Trans. Mag.* **MAG-17** (1981) 2285.
8. J. CASLAW, *Cryogenics* **11** (1971) 57.
9. M. SUENAGA and W. JANSEN, *Appl. Phys. Lett.* **43** (1983) 791.
10. R. M. SCANLAN, W. A. FIETZ and E. F. KOCH, *J. Appl. Phys.* **46** (1975) 2244.
11. D. B. SMATHERS, K. R. MARKEN, D. C. LABALESTIER and R. W. SCANLAN, *IEEE Trans. Mag.* **MAG-19** (1983) 1417.
12. B. GŁOWACKI and J. PISKORSKI, *Inzynieria Materialowa* **4** (1982) 358.
13. *Idem, ibid.* **2** (1984) 36.
14. L. M. BASLEY, C. Q. ZHANG, E. C. HARRIGAN and A. SZMYRKA, *Cryogenics* **26** (1986) 413.
15. R. POWELL and A. CLARK, *Cryogenics* **16** (1978) 137.
16. R. HAKE, *Phys. Rev.* **158** (1967) 356.
17. B. GŁOWACKI and J. CHOJCAN, *Mater. Sci.* **9** (1983) 25.

18. A. TAYLOR "X-ray Metallography" (Wiley, New York, 1961) p. 787.
19. G. RUPP, in "Filamentary Al₅ Superconductors", edited by M. Suenaga and A. F. Clark (Plenum Press, New York, 1980) p. 155.
20. K. KWASNITZA, A. V. NARLIKAR, H. U. NISSEN and D. SALATHE, *Cryogenics* **20** (1980) 715.
21. H. ULLMAYER, "Irreversible Properties of Type II Superconductors" (Springer-Verlag, Berlin, 1975) p. 146.
22. M. N. KLOPKIN, *Zh. Eksp. Teoret. Fiz.* **90** (1986) 286.
23. T. P. ORLANDO, E. J. McNILL, S. FONER and M. R. BASLEY, *Phys. Rev. B.* **19** (1979) 4545.
24. R. ESOMEKH, C. G. CUI and J. E. EVETTS, *J. Low Temp. Phys.* **50** (1983) 33.

*Received 7 August 1985
and accepted 5 June 1986*